

On axially symmetric solitons in Abelian-Higgs models

C G Doudoulakis

Department of Physics and Institute of Plasma Physics, University of Crete;
Heraklion, Crete, Greece

Abstract

A numerical search for bosonic superconducting static vortex rings in a $U(1)_A \times U(1)_W$ model is presented. The fate of these rings without current, is to shrink due to their tension until extinction. The superconductivity of the loop does not seem to prevent shrinking. Current quenching takes place before stabilization.

1 Introduction

In a series of papers [1][2] classically stable, metastable quasi-topological domain walls and strings in simple topologically trivial models, as well as in the two-higgs Standard Model (2HSM) were studied. They are local minima of the energy functional and can quantum mechanically tunnel to the vacuum, not being protected by an absolutely conserved quantum number. In [3] a search for spherically symmetric particle like solitons in the 2HSM with a simplified higgs potential was performed without success. Although the existence of spherically symmetric particle-like solitons in the 2HSM has not been ruled out, we shall here look, instead, for axially symmetric solutions in a similar system.

Consider a model with superconducting strings [2][4]. Take a piece of such string, close it to form a donut-shaped loop and let current in it. A magnetic field due to the supercurrent will be passing through the hole of the donut (fig.1). The energy of the loop has, a term proportional to the length of the string and will tend to shrink the radius of the donut to zero and the ring to extinction. However, another force opposes this tendency. Namely, as the loop shrinks, the magnetic field lines are squeezed in the hole, since, due to the Meissner effect, they cannot leave the loop. They are trapped inside the hole of the donut, oppose further shrinking and might even stabilize the string.

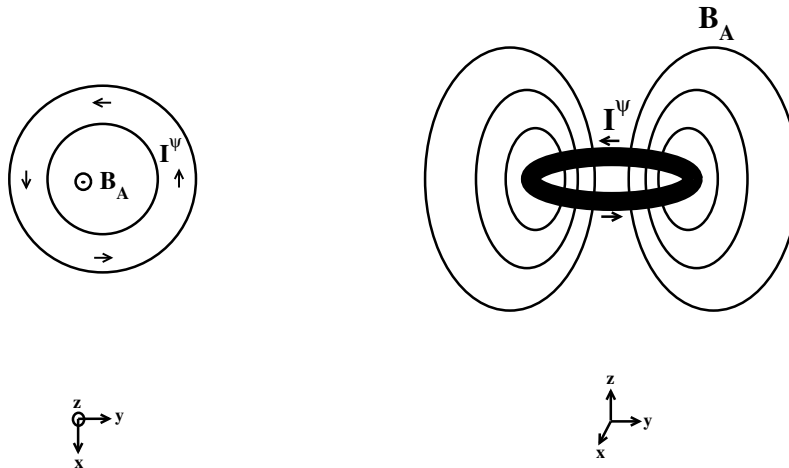


Figure 1: A $x - y$ profile of the superconducting ring (left) as well as a $y - z$ profile (right) where one can view how the mechanism we propose, against shrinking, works.

This, as well as other arguments [7] are inspiring but not conclusive. The magnetic field will not be trapped inside the loop if the penetration depth of the superconductor is larger than the thickness of the ring. Also, once the magnetic field gets strong it can destroy superconductivity and penetrate [11]. Further, there is a maximum current a superconductor can support (current quenching). This sets a limit on the magnetic field one can have through the loop, and this may not be enough to stabilize it. Thus, the above approach may work at best in a certain region of the parameter space, depending also on the defect characteristics [2]. The purpose of this work is to apply the above straightforward idea to search for string loops in a $U(1) \times U(1)$ gauge model and to determine the parameter space, if any, for their existence and stability. Another interesting subject is to have a rotating ring. The rotation is another extra factor which could help the ring to stabilize. This work was done with success both analytically and numerically on [6] where vortons are exhibited. Another recent example of rotating superconducting electroweak strings can be found on [8], while for a review on electroweak strings, the reader should also check [9]. Finally, a work on static classical vortex rings in $SU(2)$ non-abelian Yang-Mills-Higgs model can be found on [10].

2 The model

The **Lagrangian** describing our system is:

$$\mathcal{L} = -\frac{1}{4}F_{\mu\nu}^2 - \frac{1}{4}W_{\mu\nu}^2 + |D_\mu\psi|^2 + |\tilde{D}_\mu\phi|^2 - U(|\phi|, |\psi|) \quad (1)$$

where the covariant derivatives are $D_\mu\psi \equiv \partial_\mu\psi + ieA_\mu\psi$, $\tilde{D}_\mu\phi \equiv \partial_\mu\phi + iqW_\mu\phi$, the strength of the fields are $F_{\mu\nu} = \partial_\mu A_\nu - \partial_\nu A_\mu$, $W_{\mu\nu} = \partial_\mu W_\nu - \partial_\nu W_\mu$, while e and q stand as the relevant $U(1)$ charges. We choose the potential U

$$U(|\phi|, |\psi|) = \frac{g_1}{4}(|\phi|^2 - v_1^2)^2 + \frac{g_2}{4}(|\psi|^2 - v_2^2)^2 + \frac{g_3}{2}|\phi|^2|\psi|^2 - \frac{g_2}{4}v_2^4 \quad (2)$$

The vacuum of this theory is $|\phi| = v_1 \neq 0$, $|\psi| = 0$ and breaks $U(1)_W \times U(1)_A \rightarrow U(1)_A$, giving non-zero mass to W . The photon field stays massless. There, $U(v_1, 0) = 0$. The vacuum manifold \mathcal{M} in this theory is a circle S^1 and the first homotopy group of \mathcal{M} is $\pi_1(\mathcal{M}) = \pi_1(S^1) = \mathbf{Z} \neq \mathbf{1}$ which signals the existence of strings. In regions where $|\phi| = 0$, the field $|\psi|$ is arranged to be non-vanishing and $U(1)_W \times U(1)_A \rightarrow U(1)_W$. Thus, $U(1)_A \rightarrow \mathbf{1}$ and one may generate an electric current flowing along regions with vanishing $|\phi|$. Hence, this theory has superconducting strings [4]. The vacuum of the theory leaves unbroken the electromagnetic $U(1)_A$. For $g_3v_1^2 > g_2v_2^2$ this vacuum is stable, while $g_1v_1^4 > g_2v_2^4$ ensures that it is the global minimum of the potential. The mass spectrum is

$$m_A = 0, \quad m_W = qv_1, \quad m_\phi^2 = g_1v_1^2, \quad m_\psi^2 = \frac{1}{2}(g_3v_1^2 - g_2v_2^2) \quad (3)$$

3 The $U(1)_A \times U(1)_W$ model: Search of superconducting vortex rings

Configurations with torus-like shape, representing a piece of a $U(1)_W \rightarrow \mathbf{1}$ Nielsen-Olesen string, closed to form a loop, are of interest in this search. Thus, we will require ϕ to vanish on a circle of radius a (the torus radius) $\phi(\rho = a, z = 0) = 0$. At infinity ($\rho \rightarrow \infty, z \rightarrow \infty$), we have the vacuum of the theory. This translates to $|\phi| \rightarrow v_1, |\psi| \rightarrow 0$. The **ansatz** for the fields is:

$$\begin{aligned} \phi(\rho, \varphi, z) &= F(\rho, z)e^{iM\Theta(\rho, z)} \\ \psi(\rho, \varphi, z) &= P(\rho, z)e^{iN\varphi} \\ \mathbf{A}(\rho, \varphi, z) &= \frac{A_\varphi(\rho, z)}{\rho} \hat{\varphi} \\ \mathbf{W}(\rho, \varphi, z) &= W_\rho(\rho, z) \hat{\rho} + W_z(\rho, z) \hat{z} \end{aligned}$$

where M, N are the winding numbers of the relevant fields and $\hat{\rho}, \hat{\varphi}, \hat{z}$ are the cylindrical unit vectors. We use cylindrical coordinates (t, ρ, φ, z) , with space-time metric $g_{\mu\nu} = \text{diag}(1, -1, -\rho^2, -1)$. We define $\Theta(\rho, z) = \arctan(z/(\rho - a))$. We work in the $A^0 = 0 = W^0$ gauge. Especially for the gauge fields, we suppose the above form based on the following reasonable thoughts: The \mathbf{W} -field is the one related to the formation of the string thus, it exists in the constant- φ plane. This means that in general its non-vanishing components will be W_ρ and W_z . The \mathbf{A} -field is the one produced by the supercurrent flowing inside the toroidal object. The current is in the φ direction thus, we in general expect the non-vanishing

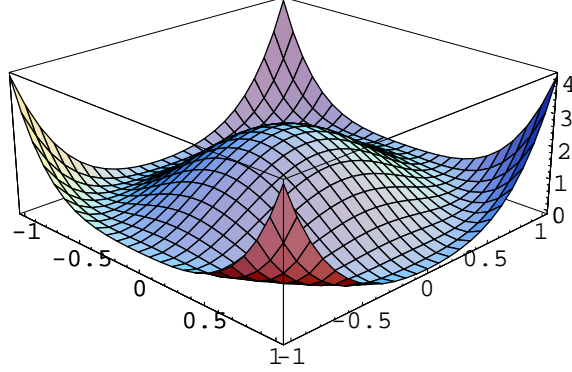


Figure 2: A wider view of the “Mexican hat” potential (eq.5) for $(g_1, g_2, u) = (10, 8, 1)$.

component to be A_φ . Finally, as it concerns the scalar fields ϕ, ψ , they follow the geometry of the toroidal defect which has axial symmetry thus, we expect that their amplitude is independent of φ .

With the above ansatz, the **energy functional** to be minimized takes the form:

$$\begin{aligned}
E = 2\pi v_1 \int_0^\infty \rho d\rho \int_{-\infty}^\infty dz & \left[\frac{1}{2\rho^2} \left((\partial_\rho A_\varphi)^2 + (\partial_z A_\varphi)^2 \right) + \right. \\
& + (\partial_\rho P)^2 + (\partial_z P)^2 + \frac{P^2}{\rho^2} (eA_\varphi + N)^2 + \\
& + (\partial_\rho F)^2 + (\partial_z F)^2 + \frac{1}{2} (\partial_\rho W_z - \partial_z W_\rho)^2 + \\
& \left. + \left((qW_\rho + M\partial_\rho \Theta)^2 + (qW_z + M\partial_z \Theta)^2 \right) F^2 + U(F, P) \right] \quad (4)
\end{aligned}$$

and the potential U can be written as follows:

$$U(F, P) = \frac{g_1}{4} (F^2 - 1)^2 + \frac{g_2}{4} (P^2 - u^2)^2 + \frac{g_3}{2} F^2 P^2 - \frac{g_2}{4} u^4 \quad (5)$$

where $u \equiv v_2/v_1$. This is the energy functional we use for our computations. The **conditions** to be satisfied by the parameters become:

$$g_1 > g_2 u^4 \quad , \quad g_3 > g_2 u^2 \quad (6)$$

The gauge fields \mathbf{A} , \mathbf{W} have **magnetic fields** of the following form:

$$\begin{aligned}
\nabla \times \mathbf{A} = \mathbf{B}_A &= \frac{1}{\rho} \left(\frac{\partial A_\varphi}{\partial \rho} \hat{z} - \frac{\partial A_\varphi}{\partial z} \hat{\rho} \right) \\
\nabla \times \mathbf{W} = \mathbf{B}_W &= - \left(\frac{\partial W_z}{\partial \rho} - \frac{\partial W_\rho}{\partial z} \right) \hat{\varphi}
\end{aligned}$$

The **field equations** follow:

$$\begin{aligned}
& \partial_\rho^2 F + \partial_z^2 F + \frac{\partial_\rho F}{\rho} - \frac{g_1}{2} (F^2 - 1) F - \frac{g_3}{2} P^2 F - \\
& \left[\left(qW_\rho - M \frac{z \cos^2 \Theta}{(\rho - a)^2} \right)^2 + \left(qW_z + M \frac{\cos^2 \Theta}{(\rho - a)} \right)^2 \right] F = 0 \\
& \partial_\rho^2 P + \partial_z^2 P + \frac{\partial_\rho P}{\rho} - (eA_\varphi + N)^2 \frac{P}{\rho^2} - \frac{g_2}{2} (P^2 - u^2) P - \frac{g_3}{2} F^2 P = 0 \\
& \partial_\rho^2 A_\varphi + \partial_z^2 A_\varphi - \frac{\partial_\rho A_\varphi}{\rho} - 2eP^2 (eA_\varphi + N) = 0 \\
& \partial_z^2 W_\rho - \partial_z \partial_\rho W_z - 2qF^2 \left(qW_\rho - M \frac{z \cos^2 \Theta}{(\rho - a)^2} \right) = 0 \\
& \partial_\rho^2 W_z + \frac{1}{\rho} (\partial_\rho W_z - \partial_z W_\rho) - \partial_\rho \partial_z W_\rho - 2qF^2 \left(qW_z + M \frac{\cos^2 \Theta}{(\rho - a)} \right) = 0
\end{aligned}$$

where $\Theta = \arctan(z/(\rho - a))$.

We can also write down the **currents** associated with ϕ field, namely j_ρ^ϕ and j_z^ϕ and the total current \mathcal{I}^ϕ out of these as well as the supercurrent \mathcal{I}^ψ associated with the ψ field. These are

$$\mathcal{I}^\phi = \sqrt{(j_\rho^\phi)^2 + (j_z^\phi)^2}, \quad \mathcal{I}^\psi = -\frac{2eP^2}{\rho} (eA_\varphi + N) \quad (7)$$

where

$$j_\rho^\phi = -2qF^2 (qW_\rho + M\partial_\rho \Theta), \quad j_z^\phi = -2qF^2 (qW_z + M\partial_z \Theta) \quad (8)$$

As explained in the Introduction, Meissner effect is of crucial importance for the stability of the torus-like object. The magnetic fields produced by the supercurrent \mathcal{I}^ψ penetrate into the toroidal defect in a distance dictated by the penetration depth. In this theory, the $U(1)_\mathbf{A}$ symmetry breaks inside the string and the photon acquires mass $m_\mathbf{A}^2 = e^2 \langle P \rangle^2$ where $\langle P \rangle$ is the expectation value of the charge condensate in the vicinity of the string core. There is the superconducting sector of the defect. The penetration depth is $\lambda = \frac{1}{m_\mathbf{A}} = \frac{1}{e\langle P \rangle}$. But $\langle P \rangle = P_{max} \leq u$ thus, one can have an estimate for λ , with a lower bound for its value. This is $\lambda \geq \frac{1}{eu}$ where the equality holds when $P_{max} = u$. On the other hand, one can also compute an upper bound for the thickness of the defect. We know that $r_\phi = \frac{1}{m_\phi} = \frac{1}{\sqrt{g_1}}$. If our concern is to search for stable rings, a reasonable step is to demand the penetration depth to be smaller than the string thickness which means

$$\lambda < r_\phi \Rightarrow \frac{1}{eP_{max}} < \frac{1}{\sqrt{g_1}} \Rightarrow e^2 P_{max}^2 > g_1 \quad (9)$$

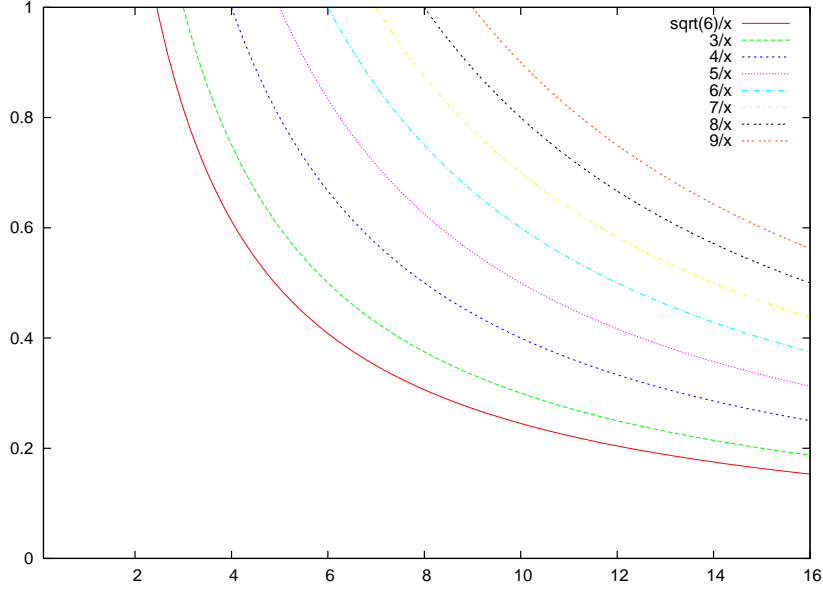


Figure 3: For different values of $\sqrt{g_1}$, we plot the lower bound over which the condition (9) is satisfied. The plot is P_{max} vs. e and we plot the function $P_{max} = \frac{\sqrt{g_1}}{e}$.

This is the condition needed in this case. From the above condition, we get the diagram shown in fig.3 where one can see the area where it's more possible to find stable solutions if they exist. The computational results we present later, are what we found while searching inside this region.

A way to produce **virial** relations is through Derrick's theorem. The virial relation for the field ϕ of our model, must have the constraint $\phi_\kappa(\rho = a, \varphi, z) = \phi(\rho = a, \varphi, z) = 0$. Consider the rescalings $\rho \rightarrow \rho$, $z \rightarrow \kappa z$, $F_\kappa \rightarrow F$, $P_\kappa \rightarrow P$, $A_{\varphi_\kappa} \rightarrow A_\varphi$, $W_{\rho, z_\kappa} \rightarrow \kappa W_{\rho, z}$. Then, we find the minimum through the relation $\frac{\partial E}{\partial \kappa} = 0$ when $\kappa = 1$. The virial relation for our model, which is a way to check

our computational results is:

$$\begin{aligned}
I_1 &= 2\pi v_1 \int_0^\infty \rho d\rho \int_{-\infty}^\infty dz \left[\frac{1}{2}(\partial_\rho W_z - \partial_z W_\rho)^2 + \frac{1}{2\rho^2}(\partial_z A_\varphi)^2 + (\partial_z P)^2 + (\partial_z F)^2 + \right. \\
&\quad \left. + 2F^2 \left(qW_\rho(qW_\rho + M\partial_\rho \Theta) + (qW_z + M\partial_z \Theta)^2 \right) \right] \\
I_2 &= -2\pi v_1 \int_0^\infty \rho d\rho \int_{-\infty}^\infty dz \left[\frac{1}{2\rho^2}(\partial_\rho A_\varphi)^2 + (\partial_\rho F)^2 + (\partial_\rho P)^2 + \frac{P^2}{\rho^2}(eA_\varphi + N)^2 + \right. \\
&\quad + (\partial_z W_\rho)(\partial_\rho W_z - \partial_z W_\rho) + F^2 \left((qW_\rho + M\partial_\rho \Theta)^2 + (qW_z + M\partial_z \Theta)^2 \right) + \\
&\quad \left. + \frac{g_1}{4}(F^2 - 1)^2 + \frac{g_2}{4}(P^2 - u^2)^2 + \frac{g_3}{2}F^2 P^2 - \frac{g_2}{4}u^4 \right]
\end{aligned}$$

and we must have $I_1 + I_2 = 0$. We define the index $V = \frac{\|I_1 - I_2\|}{\|I_1 + I_2\|}$ and we want its value to be as small as possible. We can produce many other virial relations by assuming generally for a field ϕ , the ‘‘double’’ rescaling $\phi(\vec{x}) \rightarrow \kappa\phi(\mu\vec{x})$ and then demanding $\frac{\partial E}{\partial \kappa}|_{\kappa=1=\mu} = 0 = \frac{\partial E}{\partial \mu}|_{\kappa=1=\mu}$. For example, consider the following rescalings $\rho \rightarrow \rho$, $z \rightarrow \mu z$, $F_\kappa \rightarrow F$, $P_\kappa \rightarrow \kappa P$, $A_{\varphi_\kappa} \rightarrow A_\varphi$, $W_{\rho,z_\kappa} \rightarrow W_{\rho,z}$. We have

$$\begin{aligned}
I_3 &= 2\pi v_1 \int_0^\infty \rho d\rho \int_{-\infty}^\infty dz \left[\frac{1}{2\rho^2}(\partial_z A_\varphi)^2 + (\partial_z P)^2 + (\partial_z F)^2 + \right. \\
&\quad \left. + 2F^2 \left(M\partial_z \Theta(qW_z + M\partial_z \Theta) \right) + \frac{1}{2}(\partial_\rho W_z - \partial_z W_\rho)^2 \right] \\
I_4 &= -2\pi v_1 \int_0^\infty \rho d\rho \int_{-\infty}^\infty dz \left[\frac{1}{2\rho^2}(\partial_\rho A_\varphi)^2 + (\partial_\rho P)^2 + (\partial_\rho F)^2 + \frac{P^2}{\rho^2}(eA_\varphi + N)^2 + \right. \\
&\quad + \partial_\rho W_z(\partial_\rho W_z - \partial_z W_\rho) + F^2 \left((qW_\rho + M\partial_\rho \Theta)^2 + (qW_z + M\partial_z \Theta)^2 \right) + \\
&\quad \left. + \frac{g_1}{4}(F^2 - 1)^2 + \frac{g_2}{4}(P^2 - u^2)^2 + \frac{g_3}{2}F^2 P^2 - \frac{g_2}{4}u^4 \right]
\end{aligned}$$

together with

$$\begin{aligned}
I_5 &= 2\pi v_1 \int_0^\infty \rho d\rho \int_{-\infty}^\infty dz \left[2(\partial_\rho P)^2 + 2(\partial_z P)^2 + \frac{2P^2}{\rho^2}(eA_\varphi + N)^2 \right] \\
I_6 &= 2\pi v_1 \int_0^\infty \rho d\rho \int_{-\infty}^\infty dz \left[g_2(P^2 - u^2)P^2 + g_3F^2 P^2 \right]
\end{aligned}$$

where, as above, we must have $I_3 + I_4 = 0 = I_5 + I_6$. These are the virial relations we use in order to check our results.

3.1 Computational results

Energy minimization algorithm is used to minimize the energy functional of (4). The algorithm is written in C. One can find details about the algorithm on page 425 of [5] but, briefly, the basic idea is this: Given an appropriate initial guess, there are several corrections to it, having as a criterion the minimization of the energy in every step. When the corrections on the value of the energy are smaller than $\sim 10^{-8}$ the program stops and we get the final results. A 90×20 grid for every of the five functions is used, that is, 90 points on ρ -axis and 20 on z . Here, we begin with fixed torus radius a . Then, the configuration with minimum energy for this a is found. Other values of a are chosen as well and the same process goes on until we plot the energy vs. the torus radius $E(a)$. It would be very interesting to find a non-trivial minimum of the energy (on $a_{min} \neq 0$), which would correspond to stable toroidal defects with radius a_{min} .

The **initial guess** (fig.4) we use for our computation is:

$$\begin{aligned}
 F(\rho, z) &= \tanh((\rho - a)^2 + z^2)^{M/2} \\
 P(\rho, z) &= \tanh(\rho^N)(1 - \tanh((\rho - a)^2 + z^2)) \\
 A_\varphi(\rho, z) &= -\frac{N}{e} \tanh\left(\frac{\xi \rho^2}{((\rho - a)^2 + z^2)^2}\right) \\
 W_\rho(\rho, z) &= \frac{Mz \cos^2 \Theta}{q(\rho - a)^2} \left(\frac{(\rho - a)^2 + z^2}{(\rho - a)^2 + z^2 + (a^2/4)}\right)^2 \\
 W_z(\rho, z) &= -\frac{M \cos^2 \Theta}{q(\rho - a)} \left(\frac{(\rho - a)^2 + z^2}{(\rho - a)^2 + z^2 + (a^2/4)}\right)
 \end{aligned}$$

where ξ a constant. This initial guess also satisfies the appropriate asymptotics

- near $\rho = 0$:

$$F \neq 0, \quad P \sim \rho^N, \quad A_\varphi \sim \rho^2 f(z) \quad (10)$$

- near $(\rho = a, z = 0)$:

$$F \sim \tilde{\rho}^{M/2}, \quad W_\rho = 0 = W_z \quad (11)$$

- at infinity:

$$\begin{aligned}
 F &\sim 1 - \mathcal{O}(e^{-\sqrt{\tilde{\rho}}}), \quad P \sim \mathcal{O}(e^{-\sqrt{\rho^2 + z^2}}) \\
 W_\rho &\sim -\frac{M}{q} \partial_\rho \Theta|_\infty + \mathcal{O}(e^{-\sqrt{\tilde{\rho}}}), \quad W_z \sim -\frac{M}{q} \partial_z \Theta|_\infty + \mathcal{O}(e^{-\sqrt{\tilde{\rho}}})
 \end{aligned} \quad (12)$$

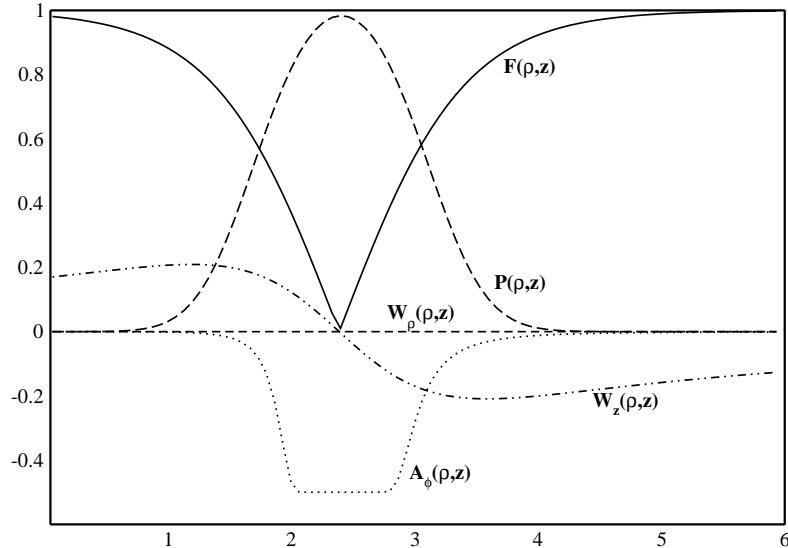


Figure 4: A typical plot of the initial guess we use for the five fields, on the lowest winding state $M = 1, N = 1$.

where $\tilde{\rho} \equiv (\rho - a)^2 + z^2$.

For fixed torus radius (i.e. here $a \approx 2.2$) we present a typical graph of the final configuration of the lowest energy (see fig.5). We also present the plot of the energy of the system vs. the radius of the toroidal object which reveals the instability of the system as there is no non-trivial minimum (see fig.8).

From the results, we can point out a few things. Firstly, the greater the value of e we use, the stronger the supercurrent becomes. Secondly, the greater the value of e we use, the lower the radius a where the supercurrent quenches (fig.6). These are expected as the increase of e makes the condition of eq.9 stronger, something which means that the mass of the photon increases and the penetration depth decreases at the same time. It is also reasonable that a stronger current can “defend” the defect, against the magnetic field, a little longer. Another observation is that as the difference $g_1 - g_2$ decreases, that is to say, as g_2 increases and becomes close to g_1 , we see that the maximum current increases and the quenching takes place again at lower a (fig.7). This is expected as one can see from the potential (eq.5) of the energy functional, because the stronger the coupling g_2 is, the more important the relevant term $g_2(P^2 - u^2)^2/4$ becomes. The latter has as a consequence, the increase of P_{max} which counteracts the effects from the increasing g_2 coupling.

The parameter space where we searched, starts from $g_1 = 4$ ($m_\phi = 2$). In order to search the model, we reached values around $g_1 = 30$ ($m_\phi \approx 5.48$) over which, e has to be very large in order to respect the condition (9). There is also the fact that great values of e in general is an unwanted feature since we use semiclassical approach. As it concerns the other couplings we have $g_3 = g_1$ and

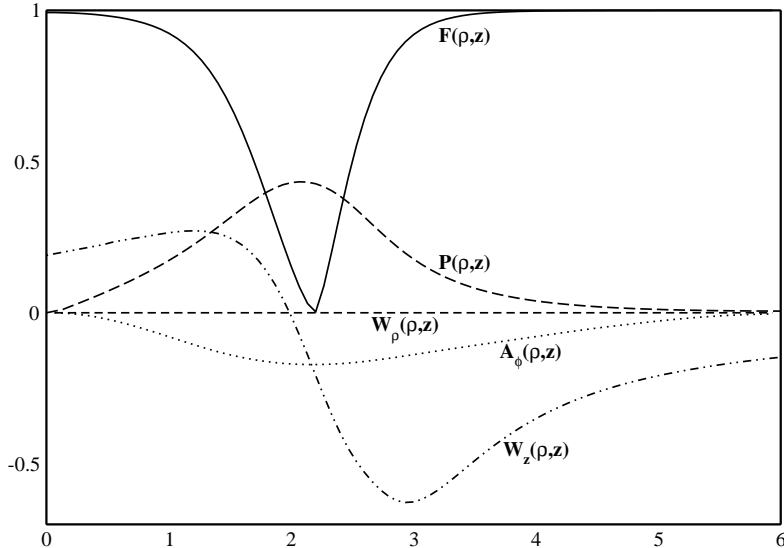


Figure 5: Typical plot of the final configuration of fields for grid 90×20 . Parameters are $M = 1$, $N = 1$, $e = 5$, $q = m_W = 2$, $g_1 = 14$, $m_\phi = \sqrt{g_1} = 3.74$, $g_2 = 12$, $g_3 = 14$, $u = 1$, $m_\psi = \sqrt{(g_3 - g_2 u^2)/2} = 1$, $v_1 = 7.5 \cdot 10^{-3}$. Energy $E = 0.72$ and virial is $1.5 \cdot 10^{-3}$.

$g_2 = g_1 - k$ with $0.5 \leq k \leq 8$, ($u = 1$).

4 Explanation concerning the instability of the vortex ring

From the condition on eq.9, it is understood that we are enforced to lower g_1 as much as possible and/or increase e . But these steps are not as easy as they might look. There are some limits. The lower bound on the value of g_1 has a reasonable explanation. For low values of g_1 , the coupling g_2 is also low (because $g_1 > g_2 u^4$). Now, when g_2 is small enough, the changes on the term $g_2(P^2 - u^2)^2/4$ are unimportant for the energy, in comparison to the term $(\partial_\rho P)^2$. In that case, the lowering of the last term minimizes the energy, something which means that $P \rightarrow 0$. Indeed, this is computationally observed. There is also a lower limit on e which is reasonable because the lowering of e results to an increasing penetration depth.

We searched for stable objects for values over these limits described above. The computational results are exhibited on figs.6-8 and as we see, these objects are unstable. We argue that the explanation for the instability is **current quenching** and that, only for high values of e . For values of e , of the order of 1, we have, according to eq.9, that the penetration depth is much bigger than the string thickness thus, stability is out of the question. The latter is also computationally observed.

Now, we base our aspect about quenching on qualitative as well as quantitative

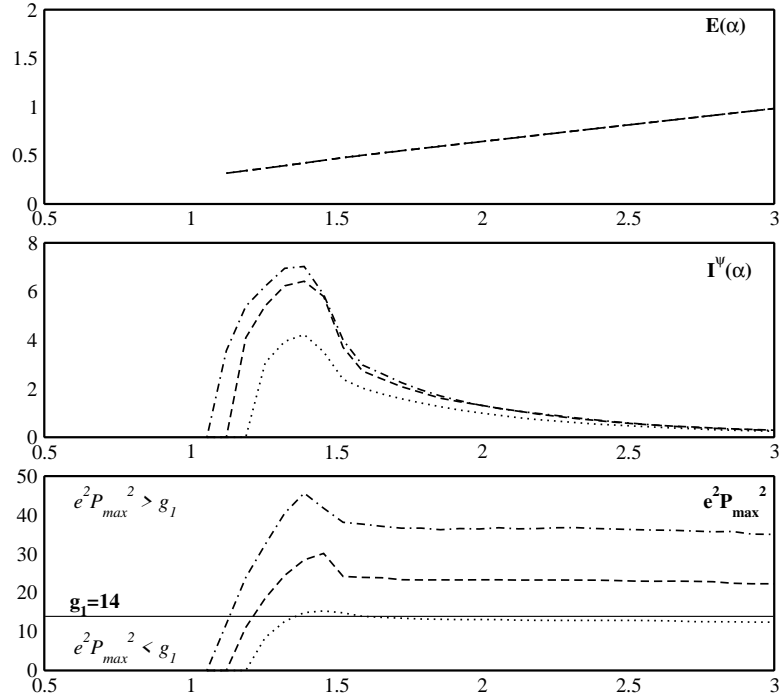


Figure 6: The top graph is the energy vs. the torus radius $E(a)$. The middle graph is the supercurrent I^ψ vs. a . On that graph one can clearly see current quenching. The bottom graph is the quantity $e^2 P_{max}^2$ vs. a (or $m_{\mathbf{A}}$ vs. a) where one can see the area in which the condition of eq.9 holds (lines over the g_1 -limit line). The resistance from the magnetic field can be seen as a sharp increase on the supercurrent. Dotted lines are for $e = 6$, dashed for $e = 8$ while dashed and dotted for $e = 10$. All plots are for $(M, N, u, g_1, g_2, g_3) = (1, 1, 1, 14, 12.5, 14)$.

arguments. We observe that as the torus shrinks, the supercurrent suddenly drops to zero which signals the destruction of the defect. Just before the sharp drop, we notice that the supercurrent rises with increasing rate. This must be due to the resistance the torus meets from the magnetic lines as it shrinks. One can observe that as the supercurrent increases and the condition of eq.9 is satisfied at the same time (i.e. see dashed and dotted line of fig.6), suddenly the current is lost. This can be explained only through current quenching. The above phenomenon is not observed when eq.9 is not satisfied (i.e. see dotted line of fig.7). There, as the magnetic lines penetrate the ring, they meet almost no resistance since λ is much greater than r_ϕ . Another observation which supports our quenching argument is that, rough estimations on the maximum current a string can sustain, lead us to the following formula (see p.129 of [11]) which makes a small overestimation in order to have an upper limit:

$$\mathcal{I}_{max}^\psi < \sigma e u \quad (13)$$

where $\sigma \equiv \int \int d\rho dz P^2$. In figs.6-7, the maximum value of the supercurrent

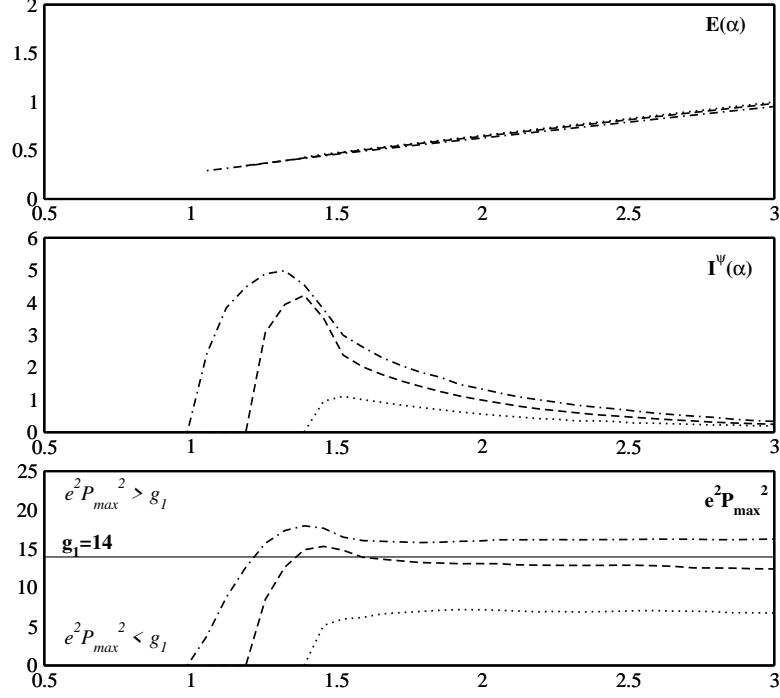


Figure 7: The top graph is the energy vs. the torus radius $E(a)$. The middle graph is the supercurrent I^ψ vs. a . On that graph one can clearly see current quenching. The bottom graph is the quantity $e^2 P_{max}^2$ vs. a (or $m_{\mathbf{A}}$ vs. a) where one can see the area in which the condition of eq.9 holds (lines over the g_1 -limit line). The resistance from the magnetic field can be seen as a sharp increase on the supercurrent. Dotted lines are for $g_2 = 12$, dashed for $g_2 = 12.5$ while dashed and dotted for $g_2 = 13$. All plots are for $(M, N, u, e, g_1, g_3) = (1, 1, 1, 6, 14, 14)$.

is close to the limit of the estimation of eq.13. The table below gathers the estimated $\mathcal{I}_{est.}^\psi$ (according to eq.13) and the computed maximum supercurrent ($\mathcal{I}_{com.}^\psi$) for the parameters of these figures.

e	g_1	g_2	g_3	$\mathcal{I}_{est.}^\psi$	$\mathcal{I}_{com.}^\psi$
6	14	12.5	14	4.6	4.3
6	14	13	14	5.2	5.0
8	14	12.5	14	6.7	6.4
10	14	12.5	14	8.0	7.2

Finally, one can make an estimation of the value of the supercurrent which would stabilize the ring, namely $\mathcal{I}_{stab.}^\psi$. This can be done as follows. As explained in the introduction, there is the tension of the string which shrinks the loop and the magnetic field which opposes this tendency. When the ring is stabilized we have $E_{tension} = E_{magnetic}$. Here, $E_{tension} \sim 1$ and $E_{magnetic} =$

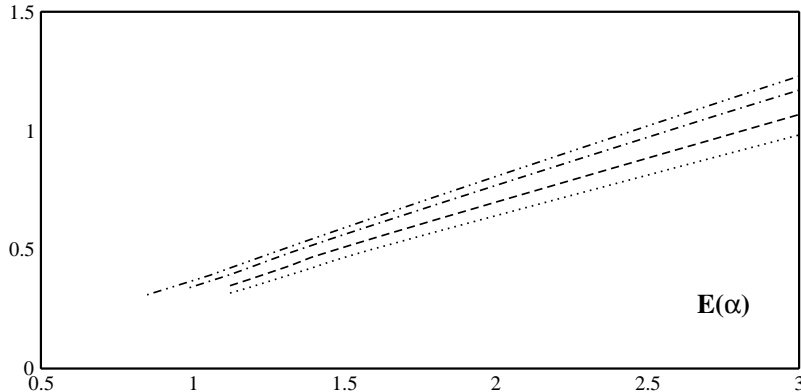


Figure 8: The plot of the energy of the system vs. the radius of the torus for four different sets of parameters. Dotted is for $(g_1, g_2, g_3)=(14, 12.5, 14)$, dashed is for $(18, 15, 18)$, dashed and dotted is for $(25, 20, 25)$ while dashed with two dots is for $(30, 24, 30)$. For all data sets we have $(e, M, N, u)=(10, 1, 1, 1)$. As one can observe, there exists no minimum.

$2\pi v_1 \int \rho d\rho \int dz (B_A^2/2)$. Without any calculation, one can point out that, since the *total* energy in the quenching radius is below $E_{tension} = 1$, then the $E_{magnetic}$ which is a fraction of it, would be even smaller. Recall that $B_A \propto \mathcal{I}^\psi$, which means that we need a \mathcal{I}_{stab}^ψ which is well above the maximum current we can have inside the defect. Calculations of the magnetic energy are in agreement with the above observation and place its value around $E_{magnetic} \sim 5 \cdot 10^{-3} \ll E_{tension} \sim 1$. This translates to the following conclusion: $\mathcal{I}_{stab}^\psi \gtrsim 10 \cdot \mathcal{I}_{est}^\psi$.

Thus, we find out that the current needed for stabilization, is at least ten times bigger than the value of the maximum current our string can sustain. We also observe that our computational maximum current values are close to the theoretical estimations about quenching. This means, that we will have current quenching as an “obstacle” towards stabilization, since the supercurrent will not be enough in order to create the magnetic field needed.

5 Conclusions

Future experiments on LHC could answer whether metastable particle-like solitons exist in MSSM or 2HSM *or* not. On [3] there is a search for spherically symmetric solitons in the frame of the 2HSM but with a simplified potential. Here we search for axially symmetric solitons which, if stable, will have a mass of few TeV [2]. We considered the $U(1)_A \times U(1)_W$ model, where the existence of the vortex is ensured, for topological reasons. There, we searched for stable toroidal strings. We present and analyse our observations. This paper tries to answer to expectations having to do with observations of stable axially symmetric solitons which would be possible to detect in later experiments of LHC. For relatively

small values of e (~ 1), the system seems to have no stable vortex rings. In fact, this instability is present even in other parameter areas where we searched (i.e. $e \geq 6$ see figs.6,7). We explain why we believe that the main reason of instability is current quenching.

6 Acknowledgments

The author is very thankful to Professor T.N.Tomaras for fruitful conversations and useful advice. Work supported in part by the ‘‘Superstrings’’ Network with EU contract MRTN-CT-2004-512194.

References

- [1] C.Bachas and T.N.Tomaras, *Nucl. Phys.* **B428** (1994) 209; conference proceedings, hep-ph/9501264; *Phys.Rev.* **D51**, 5356 (1995); *Phys.Rev.Lett.* **76**, 356 (1996); C.Bachas, B.Rai and T.N.Tomaras, *Phys.Rev.Lett.* **82**, 2443 (1999); T.N.Tomaras in conference proceedings, hep-ph/9612341; hep-ph/9707236; Y.Brihaye and T.N.Tomaras, *Nonlinearity* 12 (1999) 867
- [2] L.Perivolaropoulos and T.N.Tomaras, *Phys.Rev.* **D62** 025012, 2000; hep-ph/9911227
- [3] C.Bachas, P.Tinyakov and T.N.Tomaras, *Phys.Lett.* **B385** (1996) 237
- [4] E.Witten, *Nucl.Phys.* **B249** (1985) 557
- [5] W.H.Press, B.P.Flannery, S.A.Teukolsky, W.T.Vetterling, ‘‘Numerical Recipes’’, p.425. Cambridge University Press 1986
- [6] Y.Lemperiere and E.P.S.Shellard, *Nucl.Phys.* **B649** (2003) 511;
- [7] R.L.Davis and E.P.S.Shellard, *Nucl.Phys.* **B323** (1989) 209; R.L.Davis, *Phys.Rev.* **D38** (1988) 3722; E.Copeland, M.Hindmarsh and N.Turok, *Phys.Rev.Lett.* **58** (1987) 1910; C.T.Hill, H.M.Hodges and M.S.Turner, *Phys.Rev.Lett.* **59** (1987) 2493; C.T.Hill, H.M.Hodges and M.S.Turner, *Phys.Rev.* **D37** (1988) 263; R.L.Davis and E.P.S.Shellard, *Phys.Lett.* **B209** (1988) 485; X.Martin and P.Peter, *Phys.Rev.* **D51** (1995) 4092; B.Carter and X.Martin, *Ann.Phys.* **227** (1993) 151; B.Carter, P.Peter and A.Gangui, *Phys.Rev.* **D55** (1997) 4647; M.Nagasawa and J.Yokoyama, *Phys.Lett.* **B345** (1995) 416
- [8] M.S.Volkov, *Phys.Lett.* **B644**, (2007), 203
- [9] A.Achucarro, T.Vachaspati, *Phys.Rept.* **327**, (2000) , 347; A.Achucarro, T.Vachaspati, *Phys.Rept.* **327**, (2000) , 427

- [10] B.Kleihaus, J.Kunz, Ya.Shnir, *Phys.Rev.***D68**, (2003), 101701
- [11] A.Vilenkin, E.P.S.Shellard, “Cosmic Strings and other topological defects”, Cambridge University Press 1994
- [12] H.B.Nielsen and P.Olesen, *Nucl. Phys.* **B61** (1973) 45
- [13] E.J.Copeland, T.W.B.Kibble, D.A.Steer, hep-ph/**9803414**
- [14] D.Haws, M.Hindmarsh, N.Turok, *Phys.Lett.***B209**, (1988), 255
- [15] R.H.Brandenberger and L.Perivolaropoulos and A.Stebbins, *Int.J.Mod.Phys.***A5**, (1990), 1633
- [16] D.P.Bennett, *Phys.Rev.***D33**, (1986), 872
- [17] N.Turok, *Phys.Lett.***B126**, (1983), 437
- [18] A.Vilenkin, Q.Shafi, *Phys.Rev.lett.***51** (1983) 1716
- [19] N.Turok, *Nucl.Phys.***B242** (1984) 520
- [20] J.Silk, A.Vilenkin, *Phys.Rev.Lett.***53** (1984) 1700
- [21] N.Turok, R.H.Brandenberger, *Phys.Rev.***D33** (1986) 2175
- [22] A.Vilenkin, *Phys.Rev.Lett.***46** (1981) 1169